Electronic Supplementary Material (ESI) for Dalton Transactions.

Self-Complementary and Narcissistic Self-Sorting of bis-Acridinium Tweezers

Henri-Pierre Jacquot de Rouville,*[a] Christophe Gourlaouen[a] and Valérie Heitz*[a]

[a]Institut de Chimie de Strasbourg UMR 7177-CNRS, Université de Strasbourg, Institut Le Bel, 4 rue Blaise Pascal, 67008 Strasbourg, France. E-mail: v.heitz@unistra.fr, hpjacquot@unistra.fr

Supporting Information

Table of Contents

1. Material and General Methods

Synthesis. THF was dried using drystation GT S100 or distilled over sodium/benzophenone before use. Anhydrous DMF was purchased from ACROS organics. Column chromatography was carried out using silica gel (Merck, silica gel 60, 63−200 or 40−63 µm). Mass spectra were obtained by using a Bruker MicroTOF spectrometer in electrospray mode (ESI). Nuclear magnetic resonance (NMR) spectra for ^1H were acquired on Bruker AVANCE 300, 400, 500 and 600 spectrometers. ^{13}C spectra were acquired on a Bruker AVANCE 500 spectrometer. ^{19}F spectra were acquired on a Bruker AVANCE 300 spectrometer. The ^1H and ^{13}C spectra were referenced to residual solvent peaks.[S1] Measures of self-diffusion coefficients were performed on a Bruker 600 MHz spectrometer-Avance III, equipped with a BBI probe (Bruker BBI probe, developing a pulse field gradient of 5 G/cm/A). The sample was thermostated at 298 K unless otherwise stipulated. Diffusion NMR data were acquired using a Stimulated Echo pulse sequence with bipolar z gradients. Limited Eddy current delay was fixed to 5 ms. The diffusion time and the duration of the gradients were optimized for each sample. A recycling delay of at least 5 s was respected between scans. UV−visible spectra were recorded on a Kontron Instruments UVIKON 860 spectrometer at 21 °C with a 1 cm path cell unless otherwise specified.

Computation

All calculations were performed with GAUSSIAN 09 Rev D.01[S2] at DFT level of theory (PBEPBE functional[S3]). All atoms were described by the def2-SVP basis set[S4]. Water was described through the PCM approximation. [S5] Grimme's corrections GD3[S6] were introduced to take into account the non-covalent interactions. All structures were fully optimized and the nature of the stationary points found was checked by frequency calculations, which prove that all were true minima. Free enthalpies were extracted from these calculations.
The non-covalent interactions[S7] were studied on the basis of the wavefunctions of the optimized geometries.

2. Structural Characterizations of the Synthesized Compounds

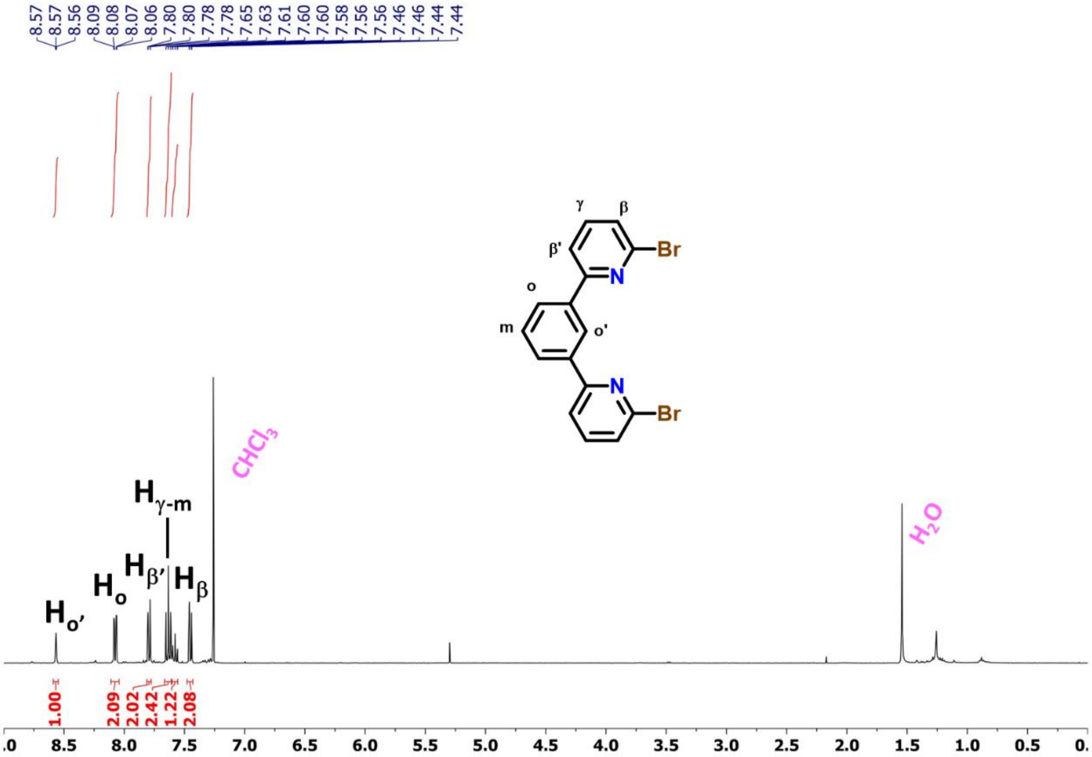

Figure S2.1: ^{1}H NMR (400 MHz, CDCl$_3$, 298 K) spectrum of **4**.

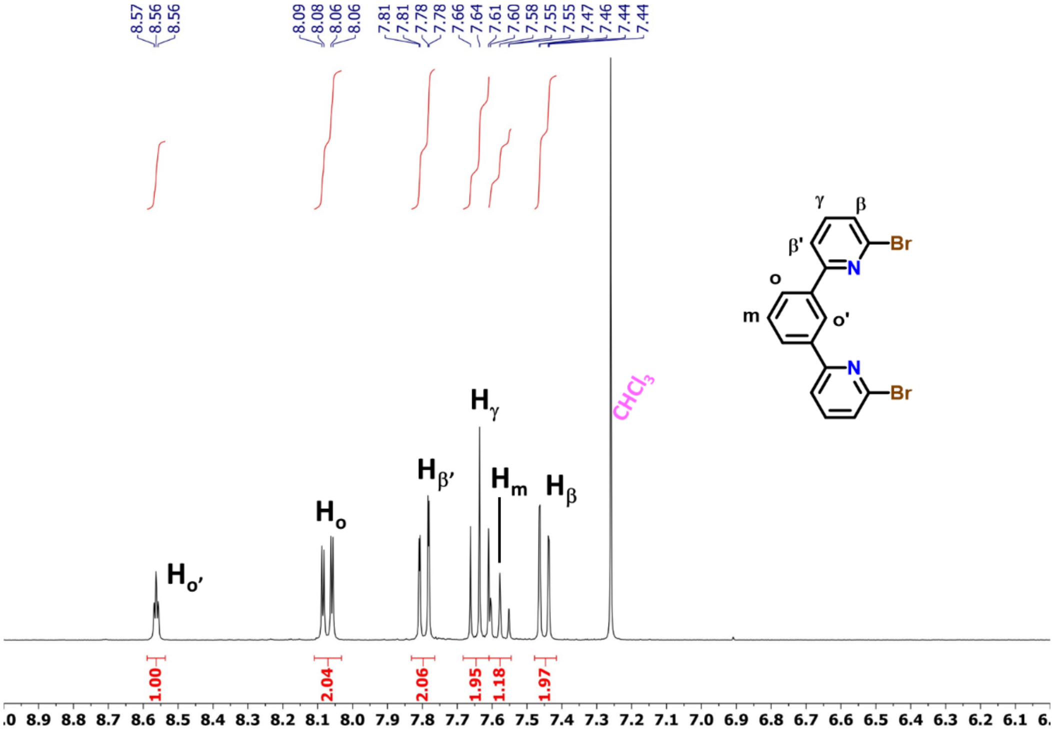

Figure S2.2: ^{1}H NMR (400 MHz, CDCl$_3$, 298 K) spectrum of **4** (zoom aromatic region).

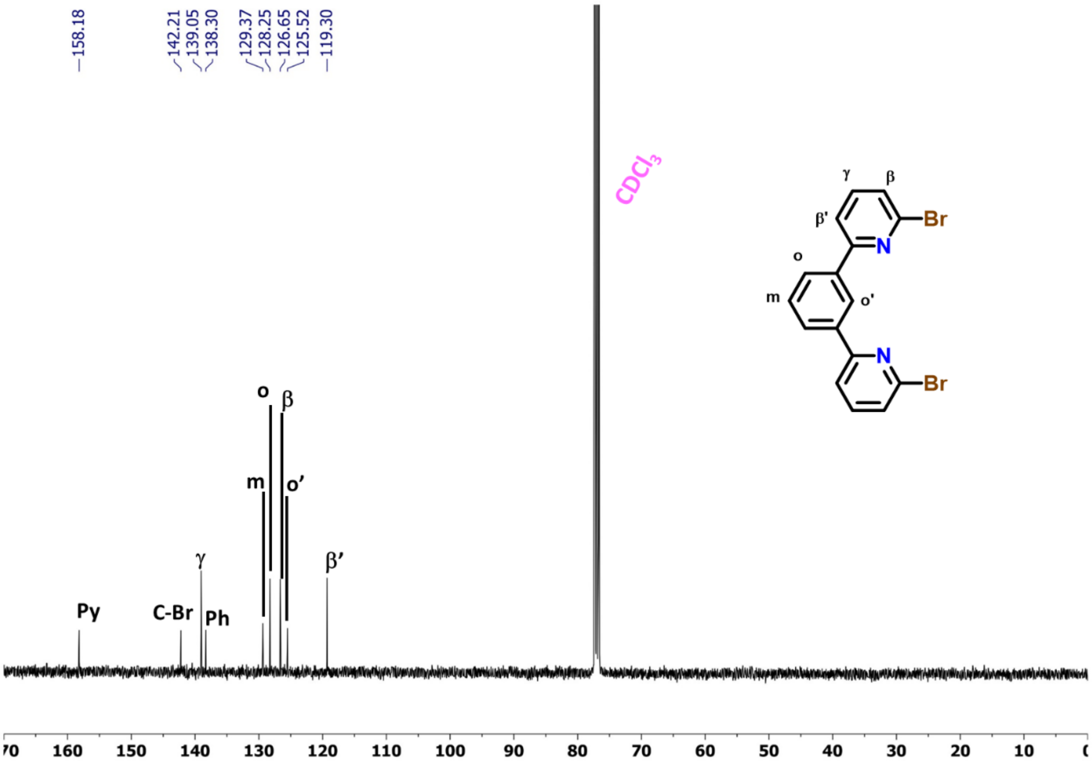

Figure S2.3: $^{13}C\{^1H\}$ NMR (100 MHz, $CDCl_3$, 298 K) spectrum of **4**.

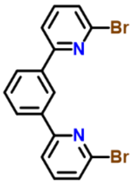

Chemical Formula: $C_{16}H_{10}Br_2N_2$
Exact Mass: 387.9211
Molecular Weight: 390.0780

Acquisition Parameter

				Set Corrector Fill	55.7 V
Source Type	ESI	Ion Polarity	Positive	n/a	n/a
n/a	n/a	n/a	n/a	n/a	n/a
Scan Begin	50 m/z	n/a	n/a	Set Reflector	1800.0 V
Scan End	3000 m/z	n/a	n/a	Set Flight Tube	8600.0 V
		n/a	n/a	Set Detector TOF	1961.2 V

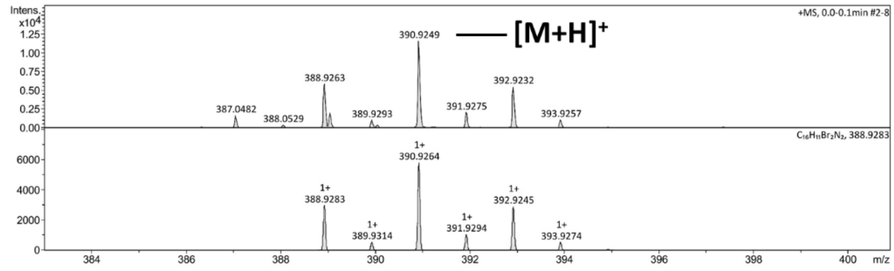

Meas. m/z	#	Ion Formula	m/z	err [ppm]	Mean err [ppm]	rdb	N-Rule	e^- Conf	mSigma	Std I	Std Mean m/z	Std I VarNorm	Std m/z Diff	Std Comb Dev
388.926293	1	C16H11Br2N2	388.928349	5.3	4.4	11.5	ok	even	10.4	9.6	n.a.	n.a.	n.a.	n.a.

Figure S2.4: HRMS (ESI-TOF) spectrum of **4**.

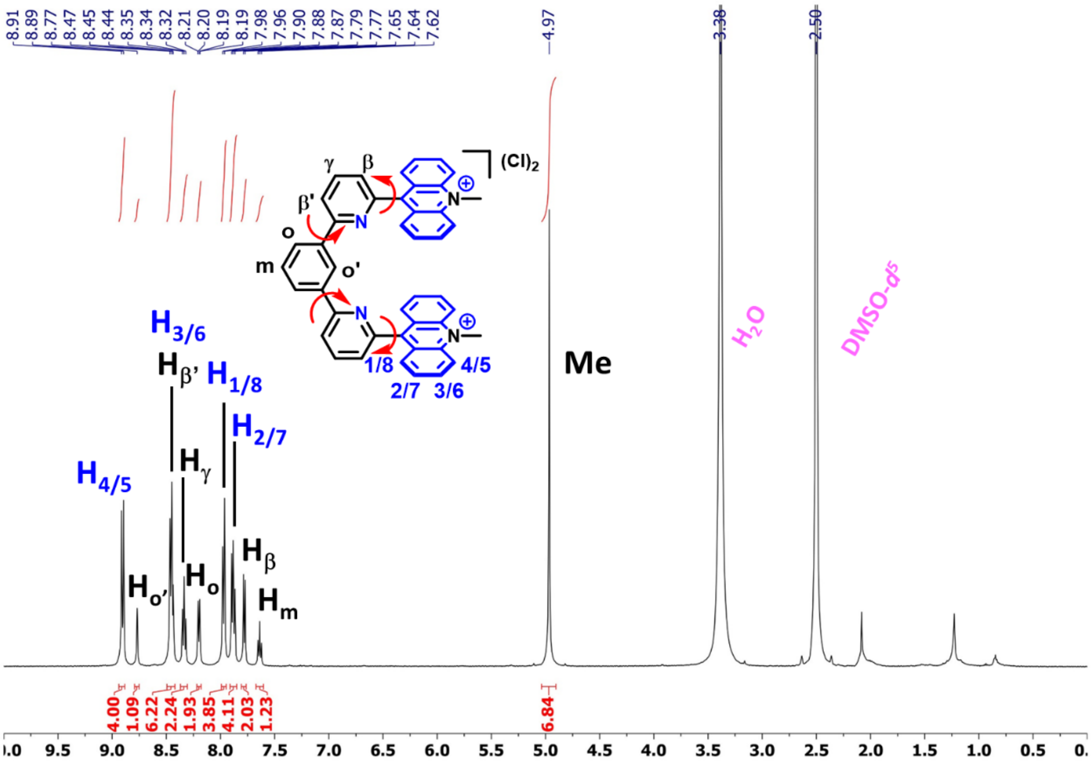

Figure S2.5: ^{1}H NMR (500 MHz, DMSO-d^6, 298 K) spectrum of **2·2Cl** (c = 1 x 10^{-2} mol L^{-1}).

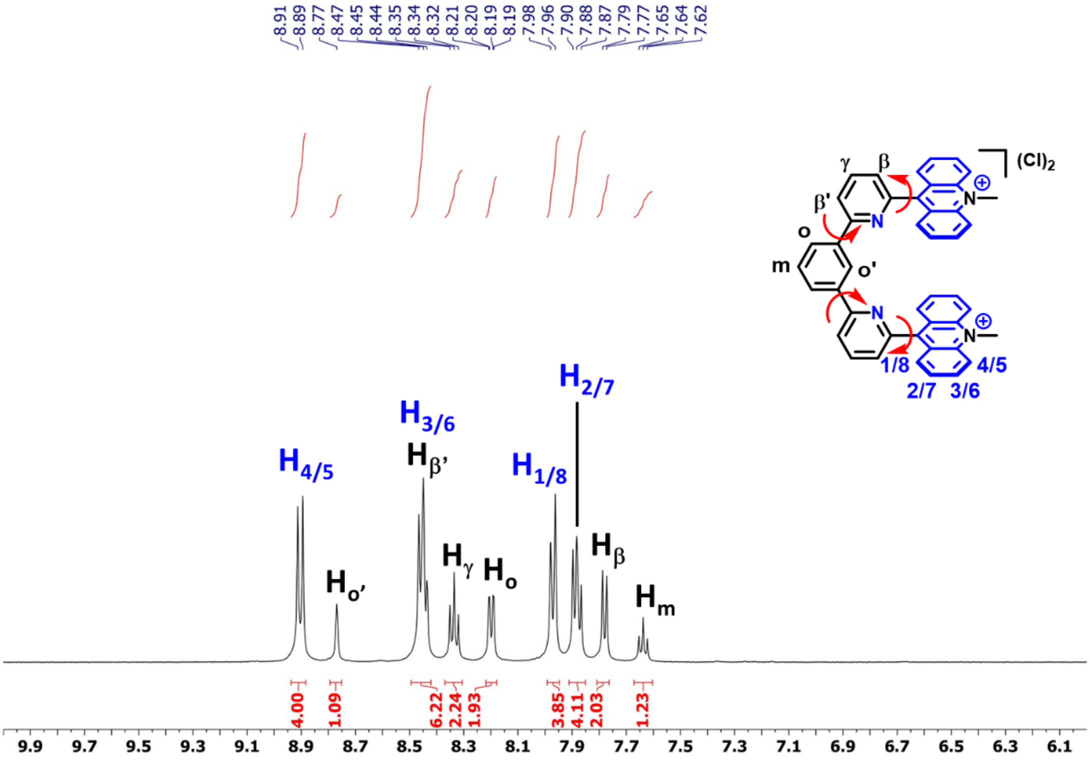

Figure S2.6: ^{1}H NMR (500 MHz, DMSO-d^6, 298 K) spectrum of **2·2Cl** (zoom aromatic region).

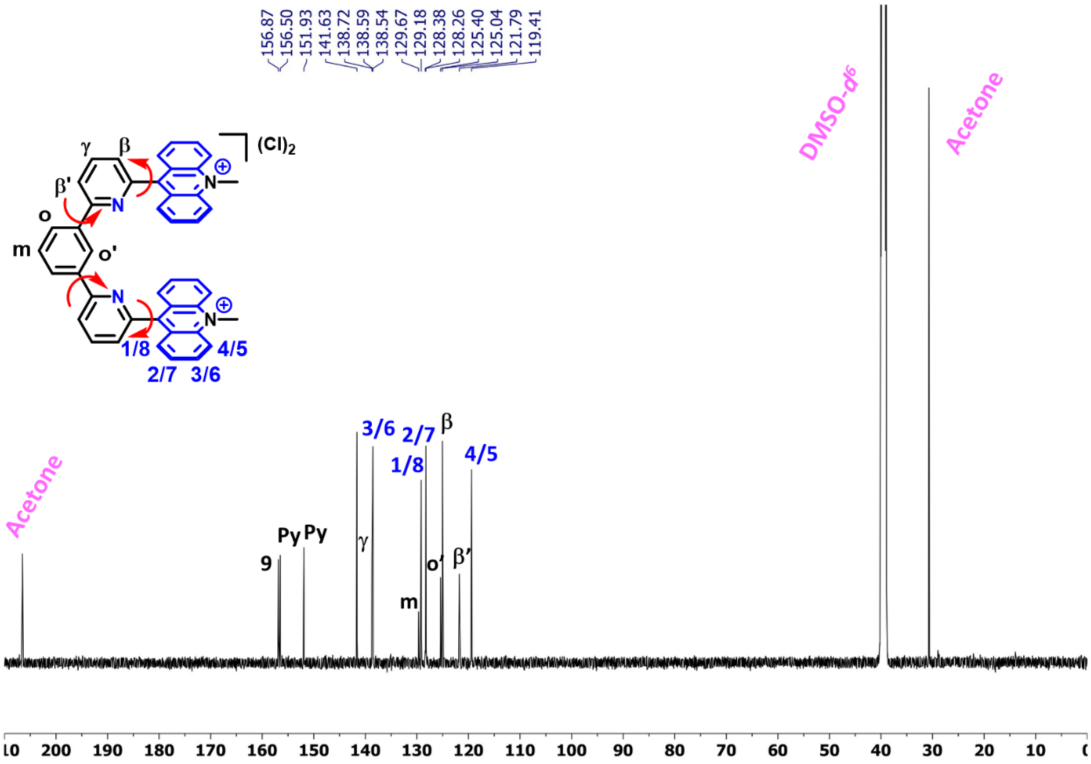

Figure S2.7: $^{13}C\{^1H\}$ NMR (125 MHz, DMSO-d^6, 298 K) spectrum of **2·2Cl** (c = 1 x 10^{-2} mol L^{-1}).

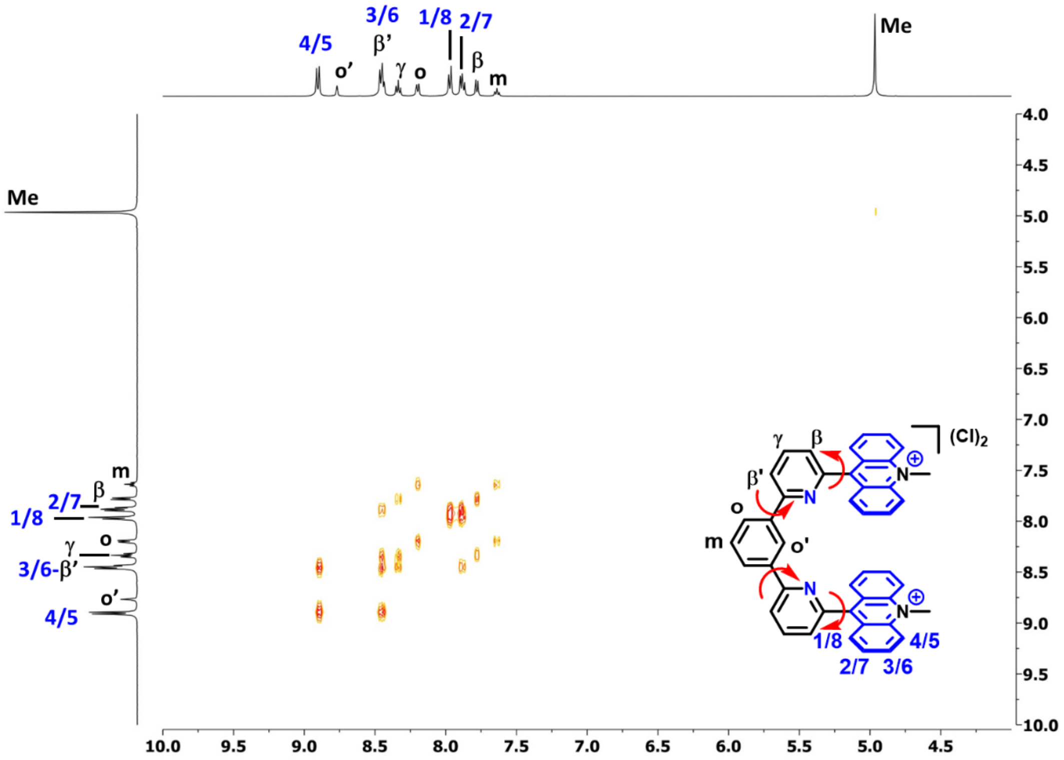

Figure S2.8: ^1H–^1H COSY 2D-spectrum (500 MHz, DMSO-d^6, 298 K) of **2·2Cl** (c = 1 x 10^{-2} mol L^{-1}).

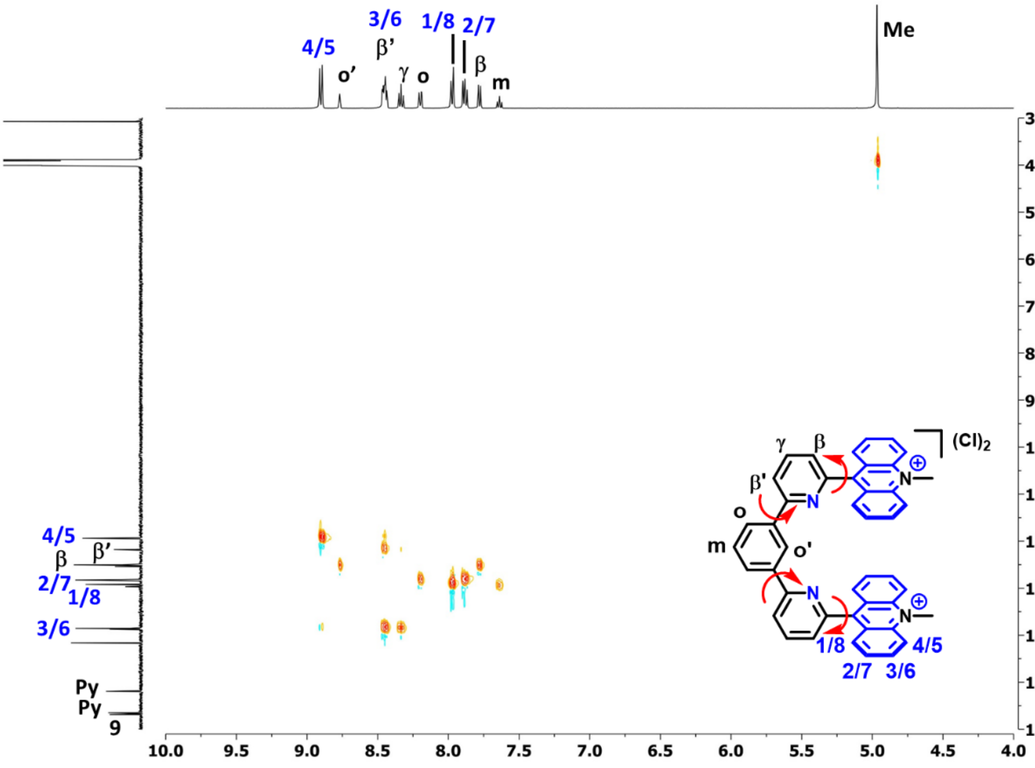

Figure S2.9: ^{1}H–^{13}C HSQC 2D-spectrum (500 MHz, DMSO-*d*^{6}, 298 K) of **2·2Cl** ($c = 1 \times 10^{-2}$ mol L^{-1}).

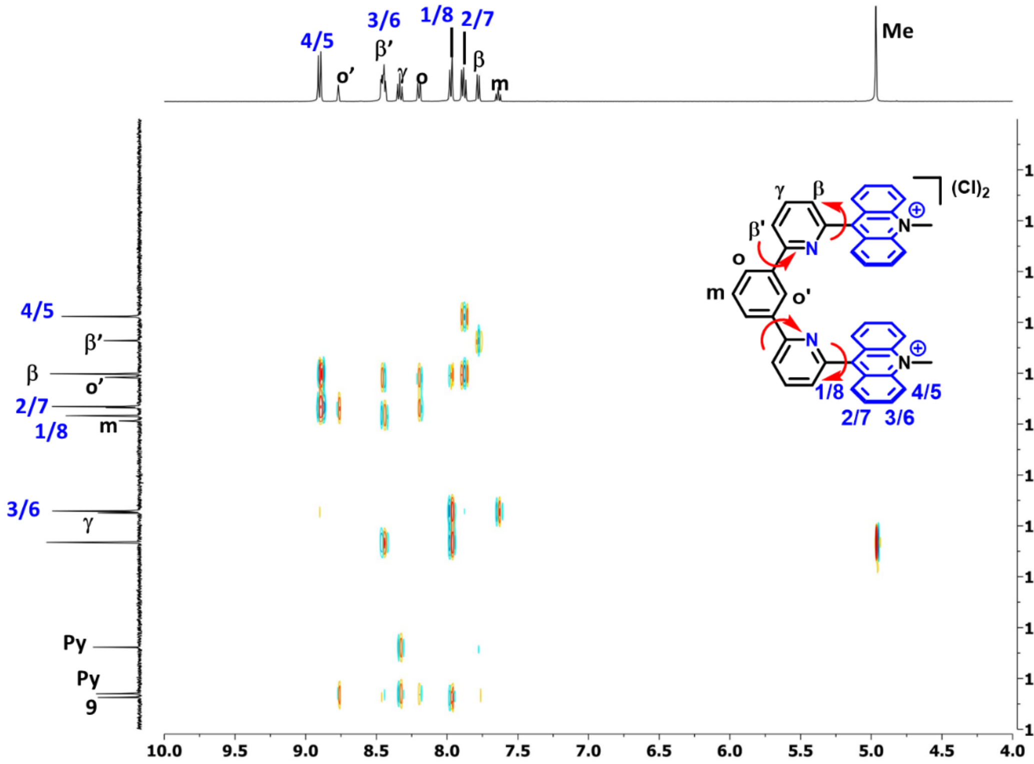

Figure S2.10: ^{1}H–^{13}C HMBC 2D-spectrum (500 MHz, DMSO-*d*^{6}, 298 K) of **2·2Cl** ($c = 1 \times 10^{-2}$ mol L^{-1}).

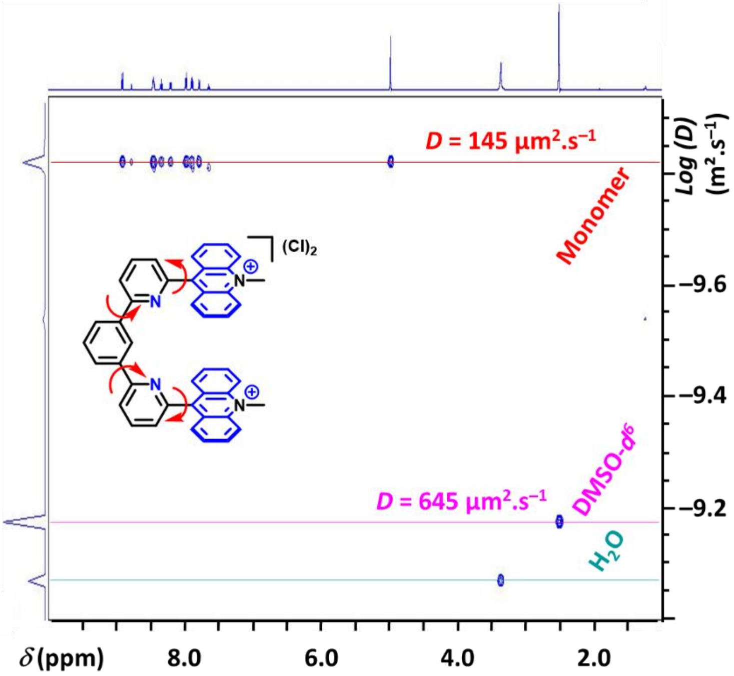

Figure S2.11: ^{1}H DOSY (600 MHz, DMSO-*d*^{6}, 298 K) spectrum of **2·2Cl** (*c* = 1 x 10^{-2} mol L^{-1}).

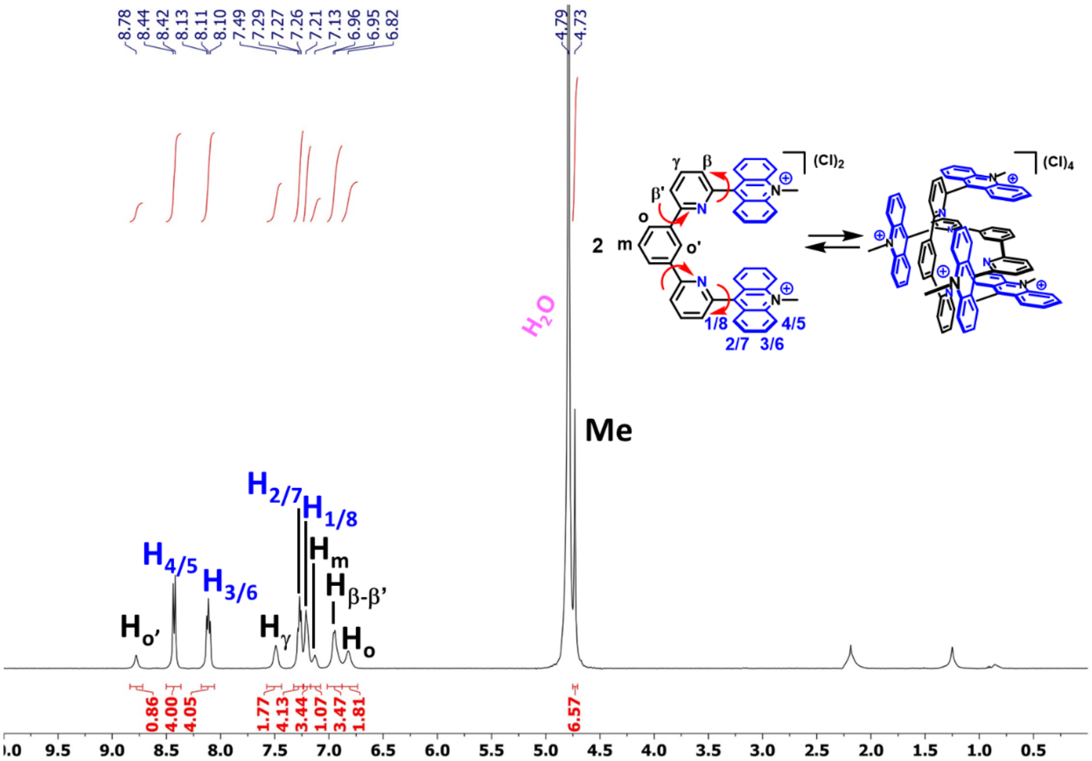

Figure S2.12: ^{1}H NMR (500 MHz, D_2O, 298 K) spectrum of **(2)$_2$·4Cl** (*c* = 1 x 10^{-2} mol L^{-1}).

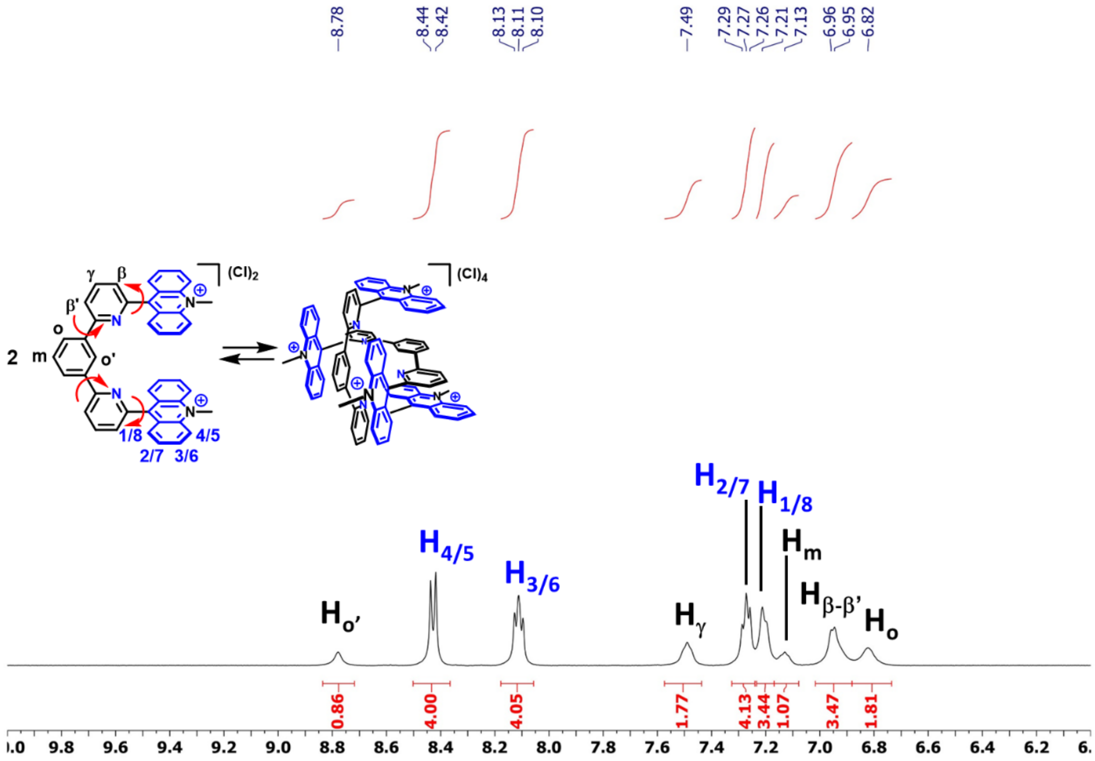

Figure S2.13: ^{1}H NMR (500 MHz, D_2O, 298 K) spectrum of **(2)$_2$·4Cl** (zoom aromatic region).

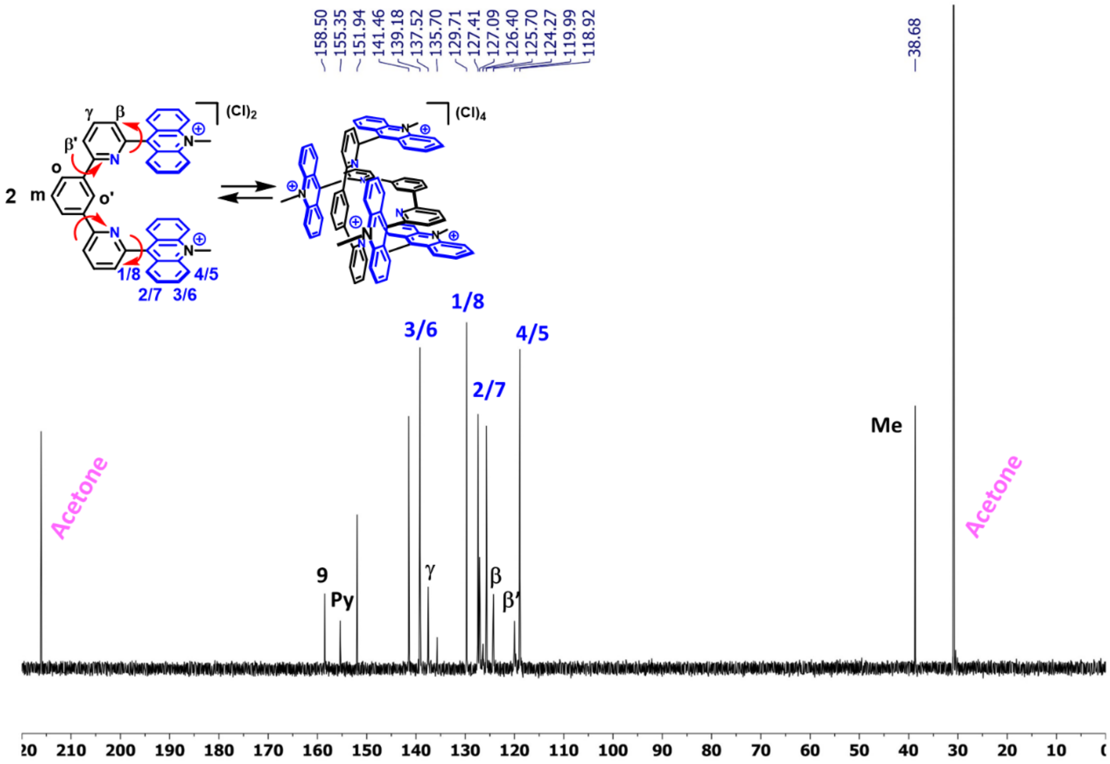

Figure S2.14: ^{13}C NMR (125 MHz, D_2O, 298 K) spectrum of **(2)$_2$·4Cl** ($c = 1 \times 10^{-2}$ mol L^{-1}).

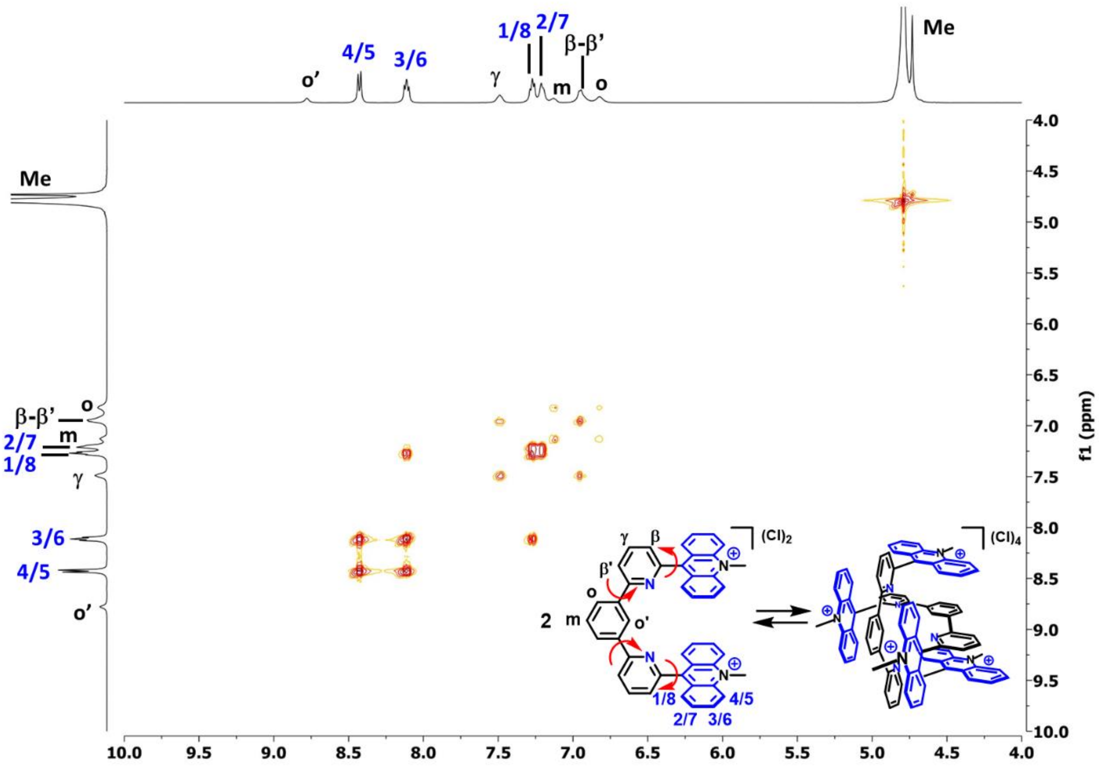

Figure S2.15: ^{1}H–^{1}H COSY 2D-spectrum (500 MHz, D_2O, 298 K) of **(2)$_2$·4Cl** ($c = 1 \times 10^{-2}$ mol L^{-1}).

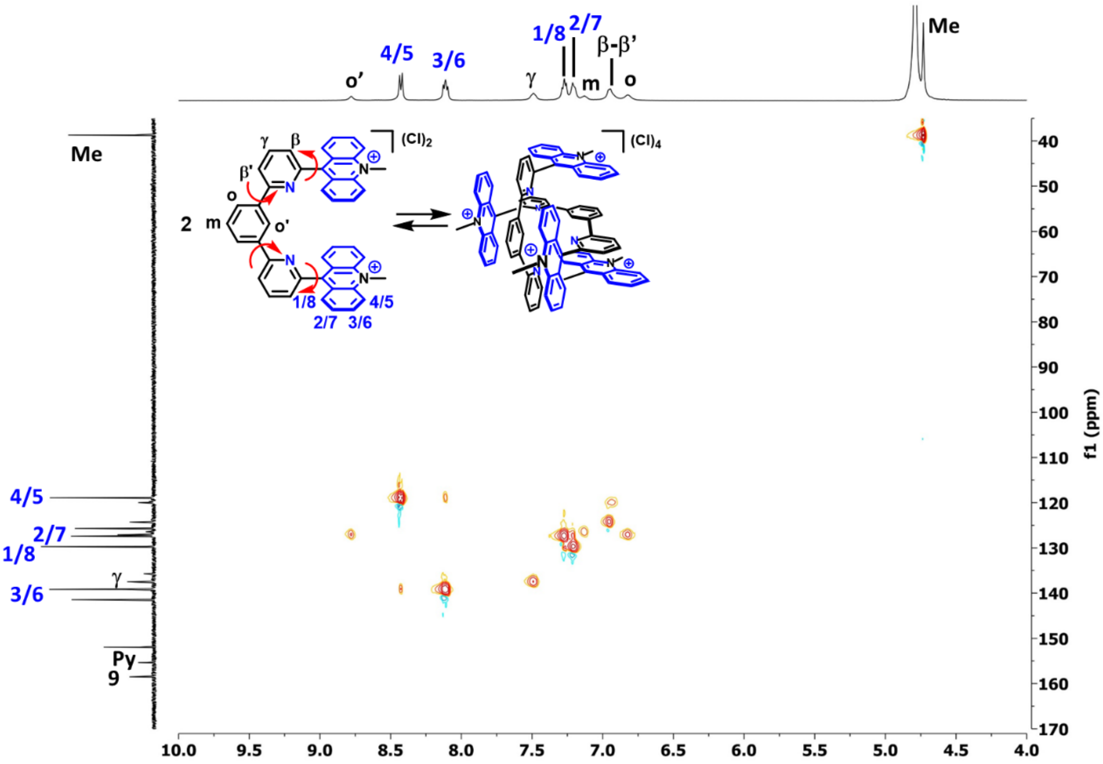

Figure S2.16: ^{1}H–^{13}C HSQC 2D-spectrum (500 MHz, D_2O, 298 K) of **(2)$_2$·4Cl** ($c = 1 \times 10^{-2}$ mol L^{-1}).

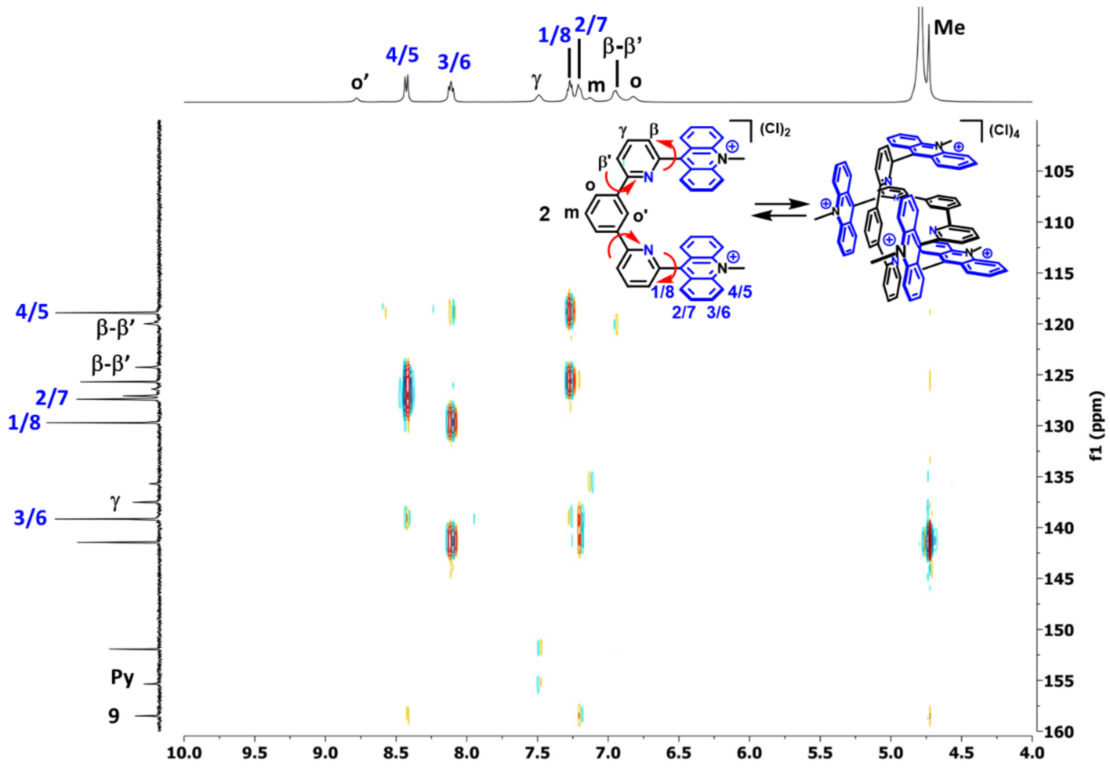

Figure S2.17: ^{1}H–^{13}C HMBC 2D-spectrum (500 MHz, D$_2$O, 298 K) of **(2)$_2$·4Cl** (c = 1 x 10^{-2} mol L^{-1}).

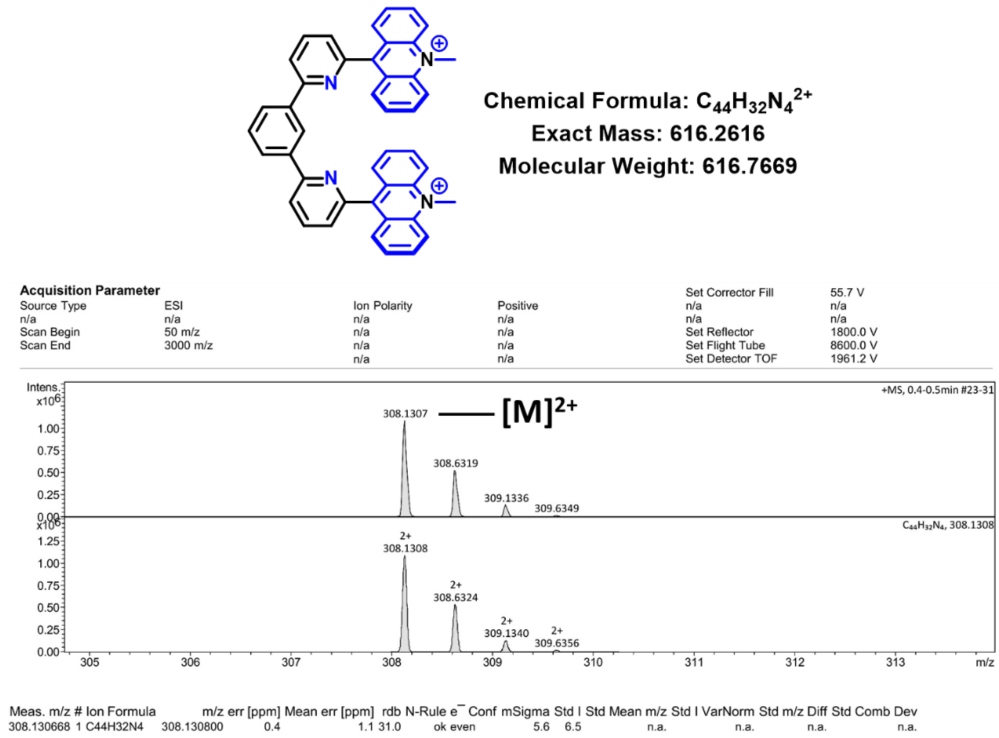

Chemical Formula: $C_{44}H_{32}N_4^{2+}$
Exact Mass: 616.2616
Molecular Weight: 616.7669

```
Acquisition Parameter                                                         Set Corrector Fill   55.7 V
Source Type     ESI            Ion Polarity     Positive                      n/a                  n/a
n/a             n/a            n/a              n/a                           n/a                  n/a
Scan Begin      50 m/z         n/a              n/a                           Set Reflector        1800.0 V
Scan End        3000 m/z       n/a              n/a                           Set Flight Tube      8600.0 V
                               n/a              n/a                           Set Detector TOF     1961.2 V
```

```
Meas. m/z # Ion Formula        m/z err [ppm] Mean err [ppm]  rdb N-Rule e¯ Conf mSigma Std I Std Mean m/z Std I VarNorm Std m/z Diff Std Comb Dev
308.130668 1 C44H32N4   308.130800       0.4              1.1 31.0     ok even        5.6   6.5         n.a.          n.a.          n.a.          n.a.
```

Figure S2.18: HRMS (ESI-TOF) spectrum of **2·2Cl**.

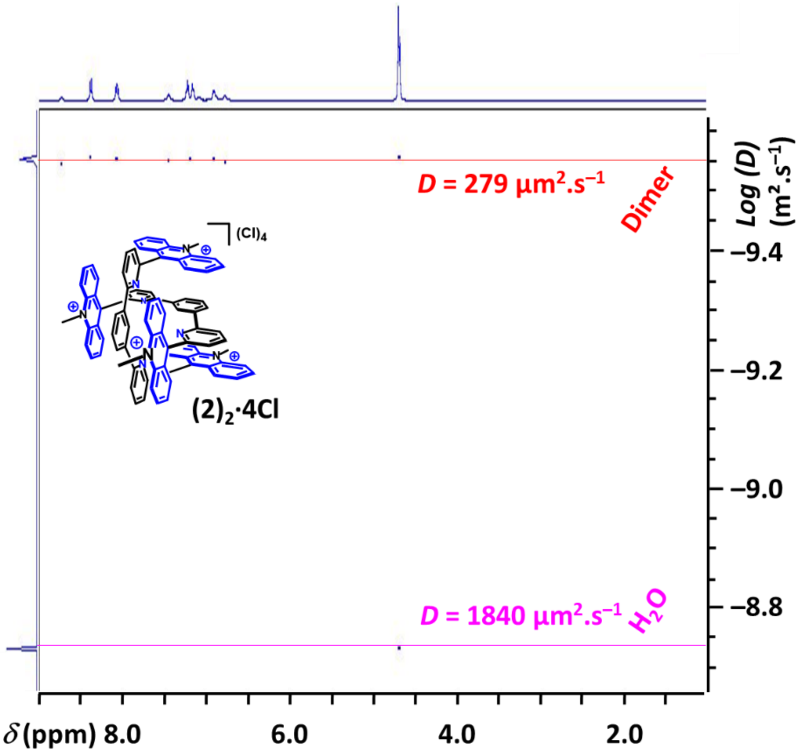

Figure S2.19: ^{1}H DOSY (600 MHz, D$_2$O, 298 K) spectrum of **(2)$_2$·4Cl** (c = 1 x 10^{-2} mol L^{-1}).

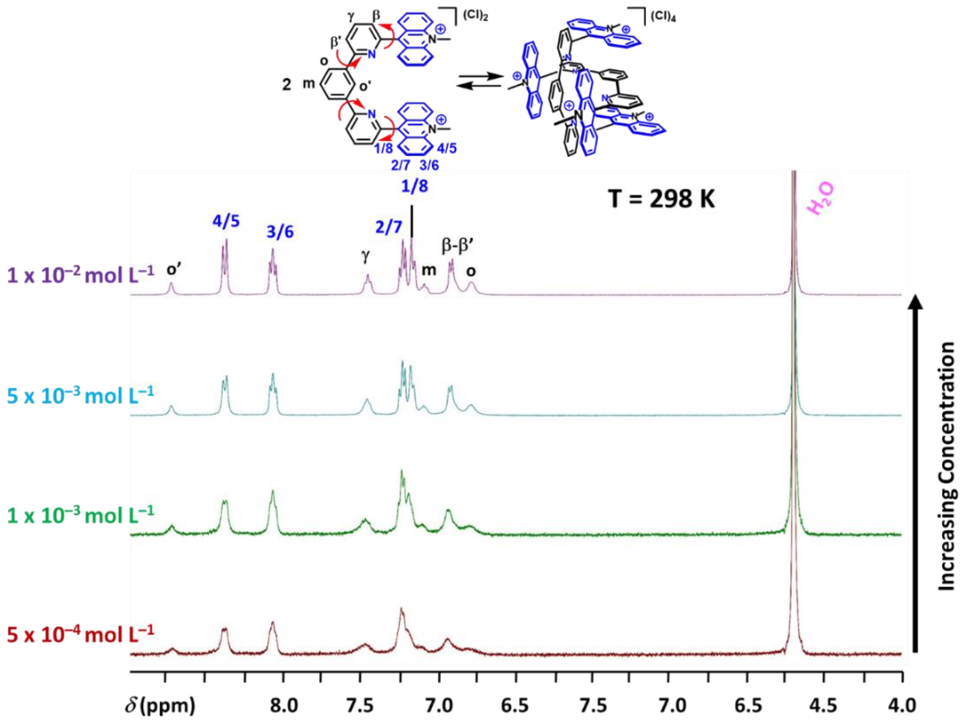

Figure S2.20: ^{1}H NMR (400 MHz, D$_2$O, 298 K) spectra of **(2)$_2$·4Cl** at 1 x 10^{-2}, 5 x 10^{-3}, 1 x 10^{-3}, 5 x 10^{-4} mol L^{-1}.

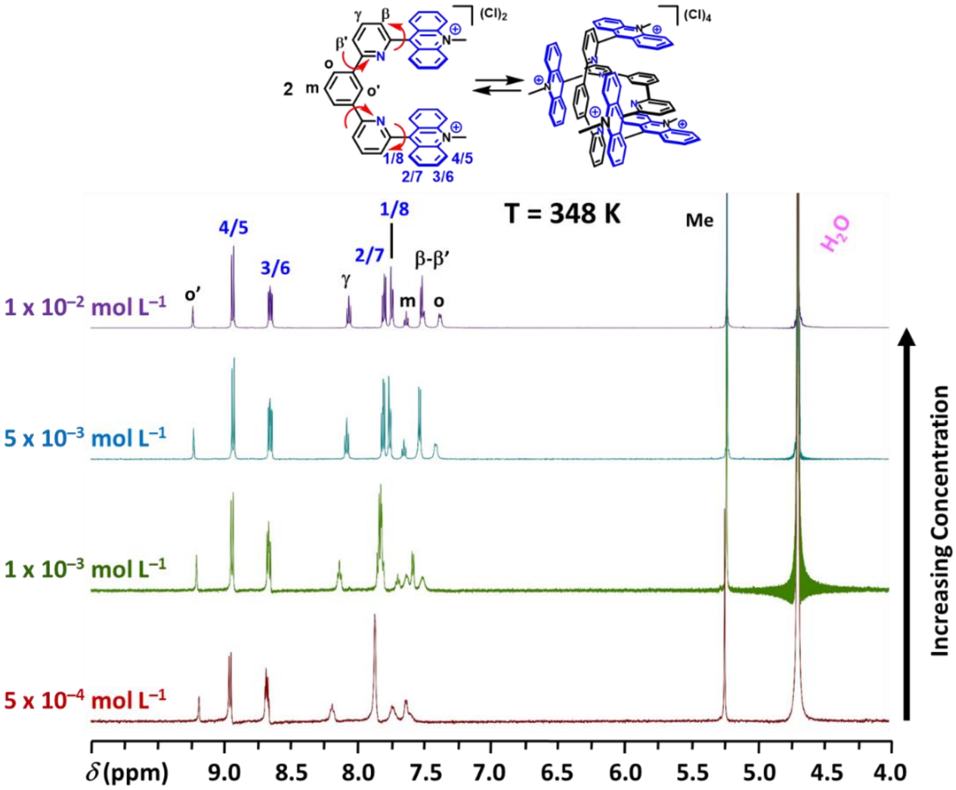

Figure S2.21: ^{1}H NMR (400 MHz, D_2O, 348 K) spectra of **(2)$_2$·4Cl** at 1 x 10^{-2}, 5 x 10^{-3}, 1 x 10^{-3}, 5 x 10^{-4} mol L^{-1}.

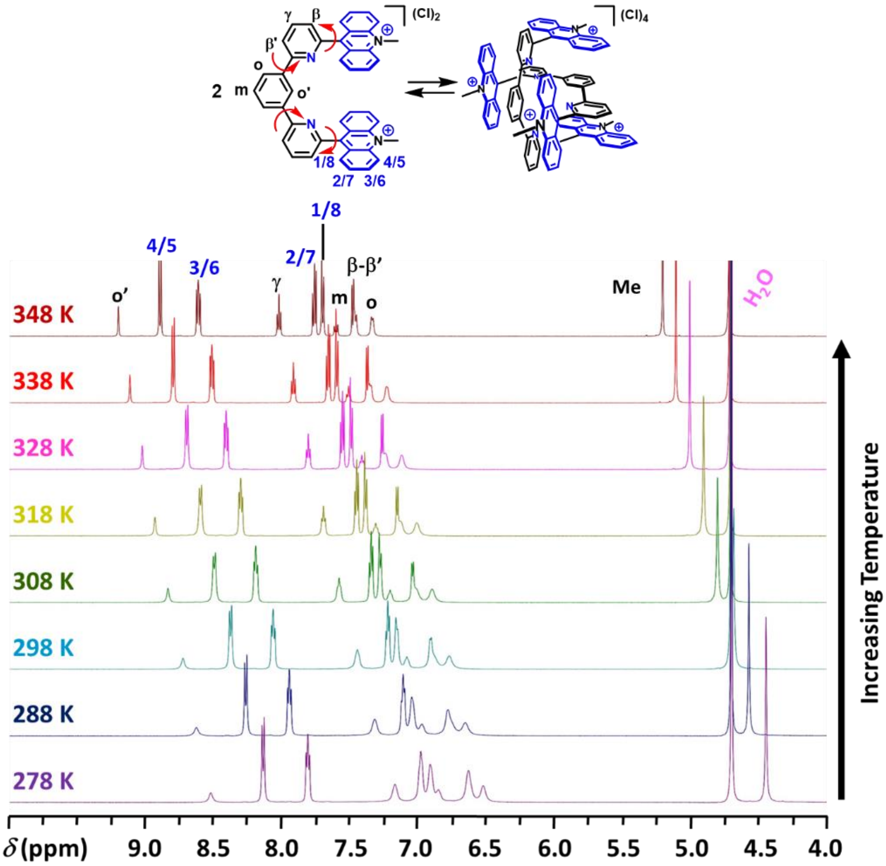

Figure S2.22: ^{1}H NMR (400 MHz, D_2O, 298 K, *c* = 1 x 10^{-2} mol L^{-1}) spectra of **(2)$_2$.4Cl** from 278 K to 348 K.

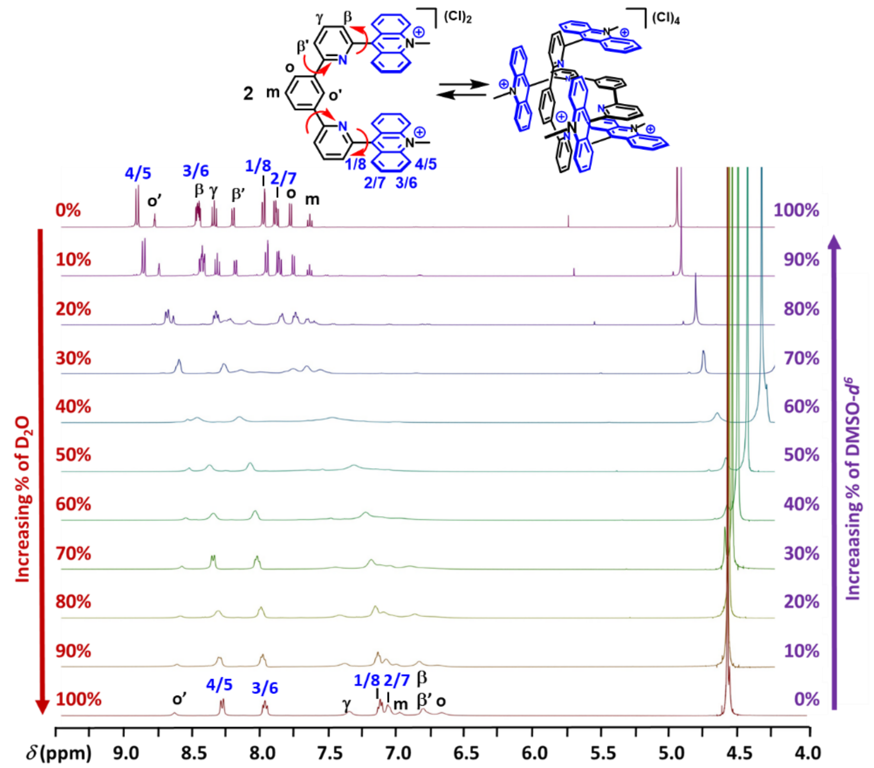

Figure S2.23: ^{1}H NMR (500 MHz, 298 K, $c = 3 \times 10^{-3}$ mol L^{-1}) spectra of **2.2Cl** from pure DMSO-d^6 to pure D_2O.

3. Self-Sorting Experiments of a Mixture of $(1)_2{\cdot}4Cl$ and $(2)_2{\cdot}4Cl$

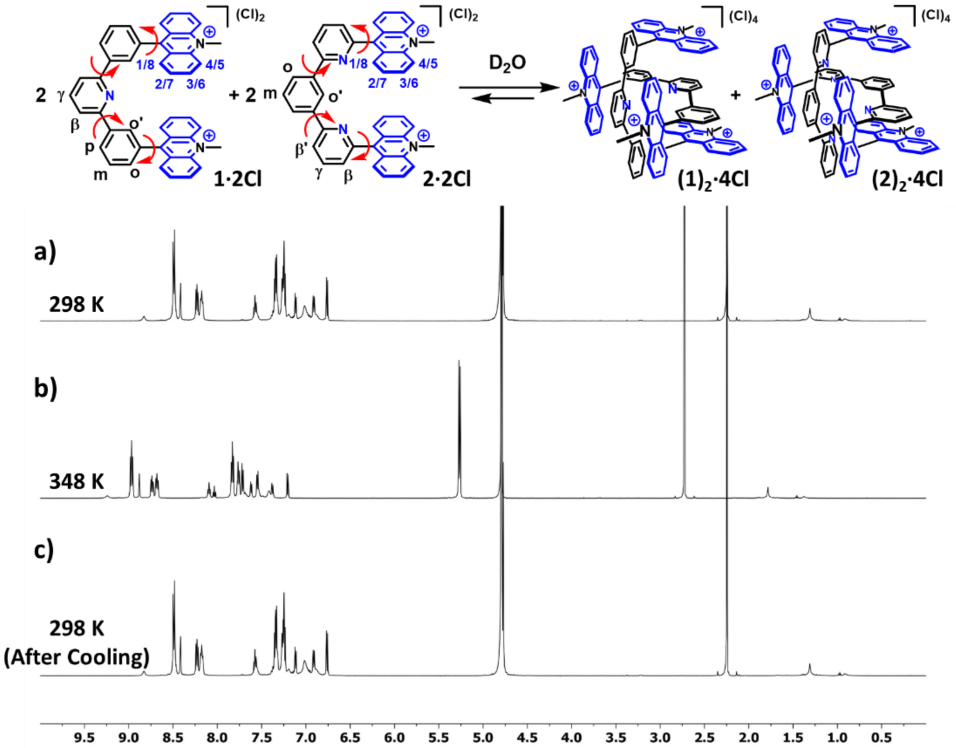

Figure S3.1: ^{1}H NMR (500 MHz, D_2O, $c = 1 \times 10^{-2}$ mol L^{-1}) spectra of a 1:1 mixture of $\mathbf{(1)_2{\cdot}4Cl}$ and $\mathbf{(2)_2{\cdot}4Cl}$ (a) at 298 K, (b) after heating up the sample at 348 K and (c) after cooling the sample back at 298 K.

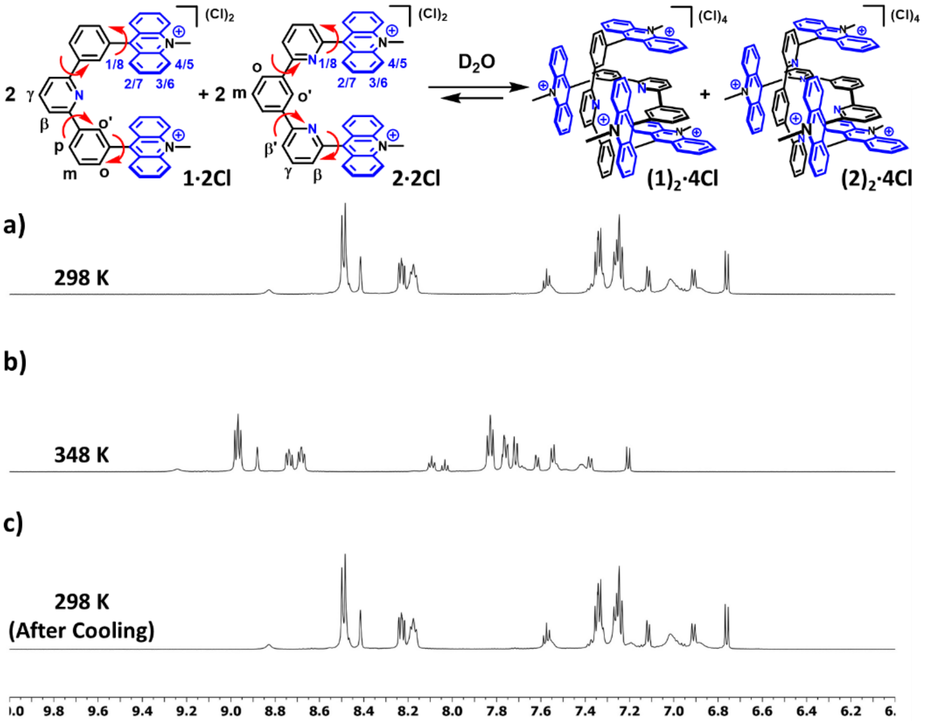

Figure S3.2: ^{1}H NMR (500 MHz, D_2O, $c = 1 \times 10^{-2}$ mol L^{-1}) spectra of a 1:1 mixture of $\mathbf{(1)_2{\cdot}4Cl}$ and $\mathbf{(2)_2{\cdot}4Cl}$ (a) at 298 K, (b) after heating up the sample at 348 K and (c) after cooling the sample back at 298 K (zoom aromatic region).

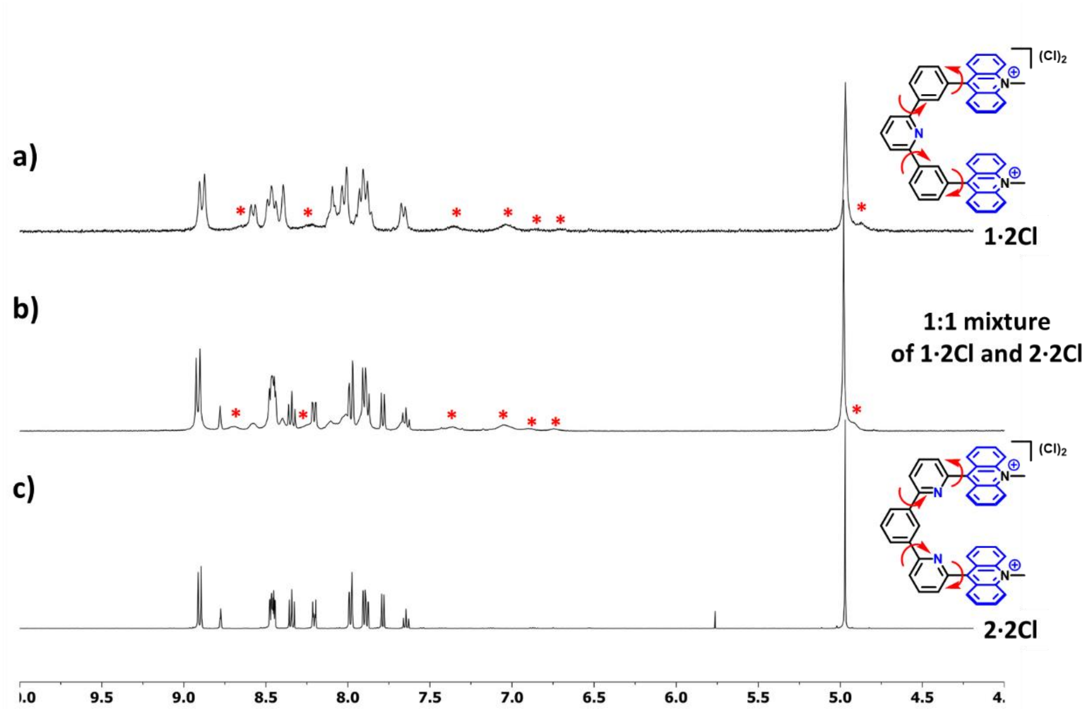

Figure S3.3: ^{1}H NMR (500 MHz, DMSO-d^6, 298 K, c = 1 x 10^{-2} mol L^{-1}) spectra (a) of **1·2Cl** (*corresponding to traces of **(1)₂·4Cl**), (b) of a 1:1 mixture of **1·2Cl** and **2·2Cl** and (c) of **2·2Cl**.

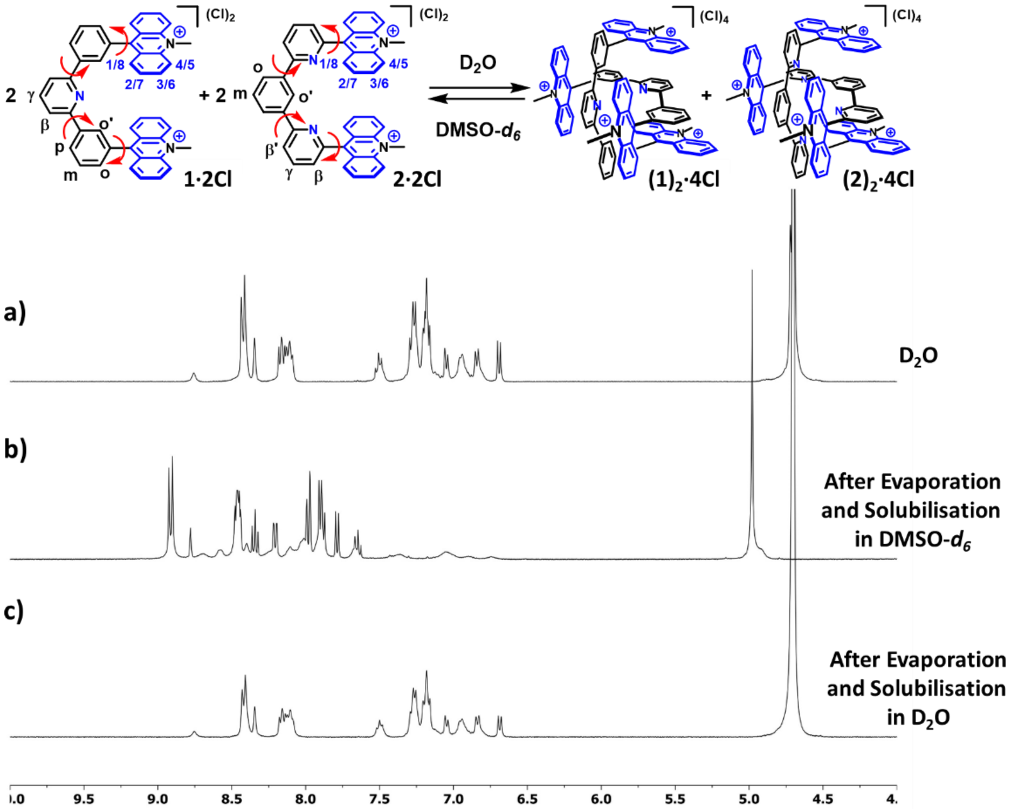

Figure S3.4: ^{1}H NMR (400 MHz, 298 K, c = 1 x 10^{-2} mol L^{-1}) spectra of a 1:1 mixture of **(1)₂·2Cl** and **(2)₂·2Cl** in (a) D_2O, (b) after successive evaporation and solubilisation in DMSO-d^6 and (c) after successive evaporation and solubilisation in D_2O.

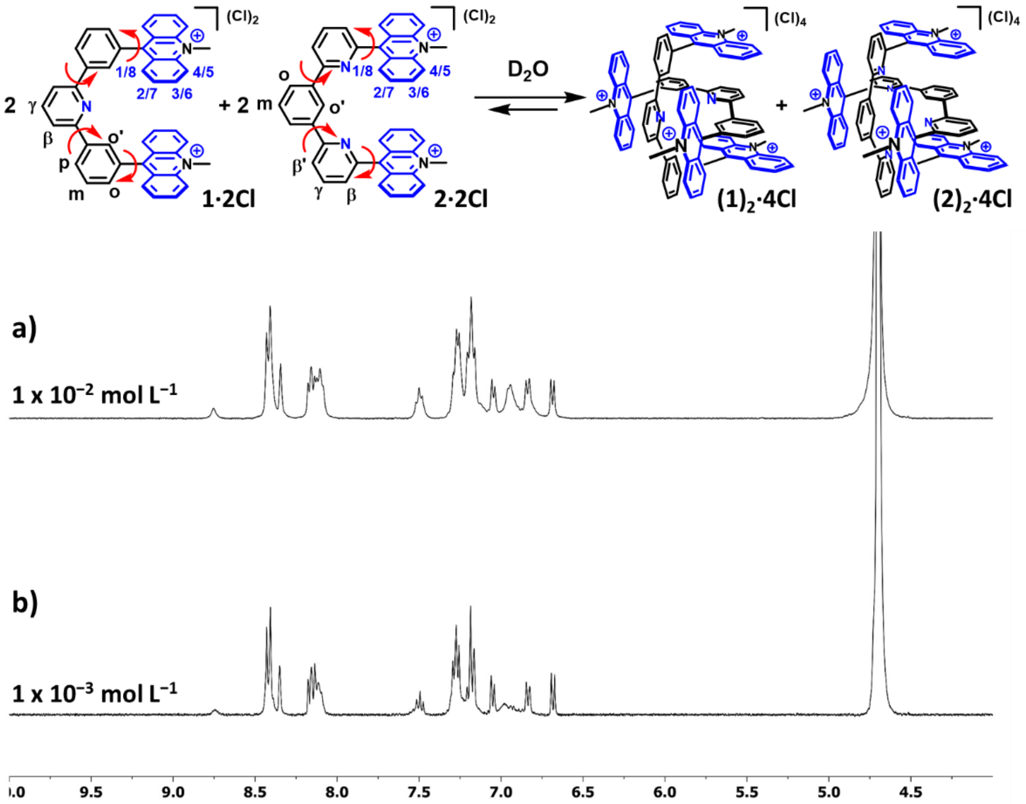

Figure S3.5: ^{1}H NMR (400 MHz, D_2O, 298 K) spectra of a 1:1 mixture of **$(1)_2$·2Cl** and **$(2)_2$·2Cl** at a concentration of (a) 1 x 10^{-2} mol L^{-1} and (b) 1 x 10^{-3} mol L^{-1}.

4. UV-Visible Characterization of 2·2Cl and $(2)_2$·4Cl

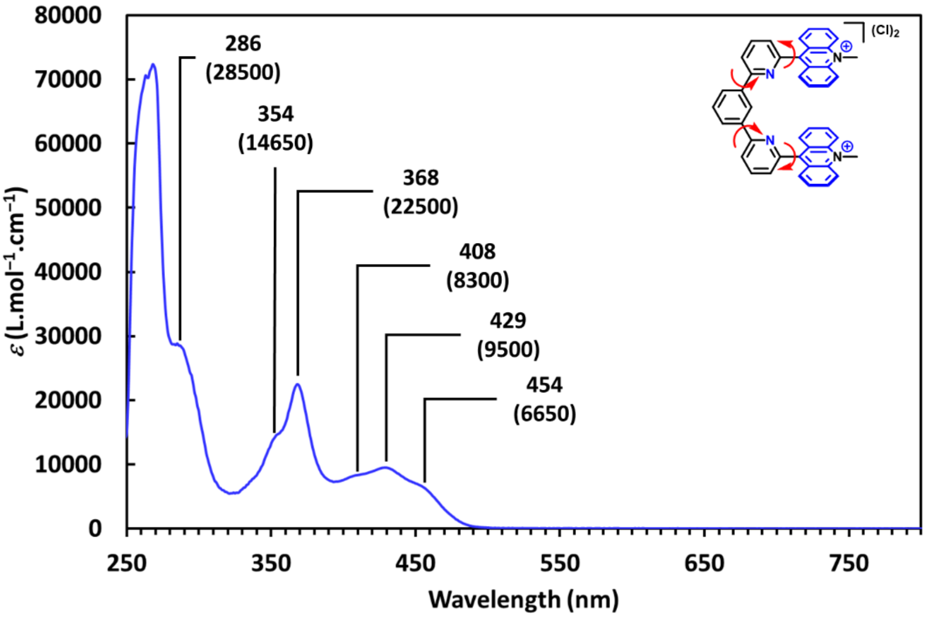

Figure S4.1: UV-Vis (DMSO, l = 0.2 cm, 298 K) spectrum of **2·2Cl** (c = 2.5 x 10^{-4} mol·L^{-1}).

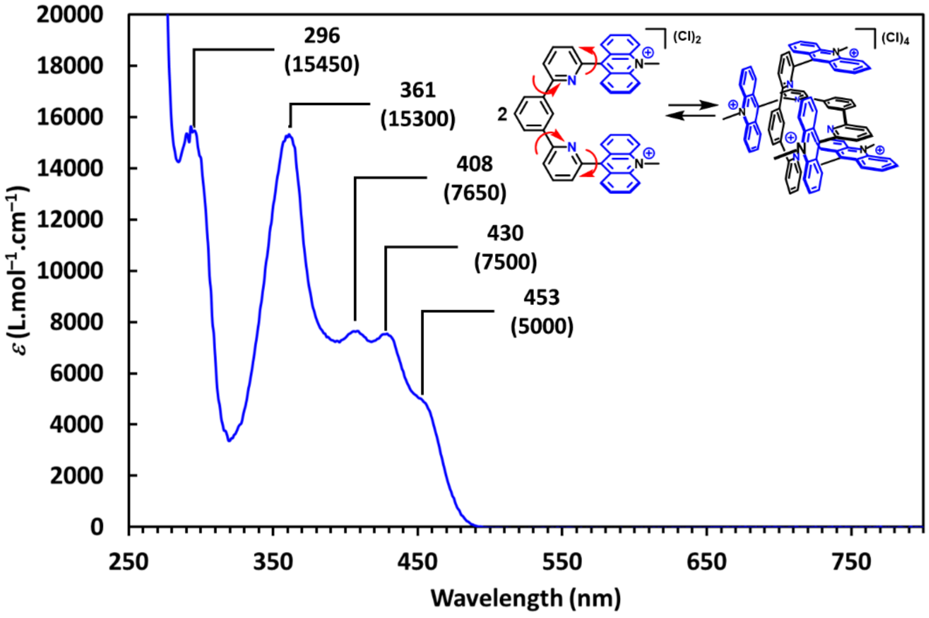

Figure S4.2: UV-Vis (H_2O, l = 0.1 cm, 298 K) spectrum of **(2)₂·4Cl** (c = 5 x 10^{-4} mol·L^{-1}).

5. Theoretical Investigation

	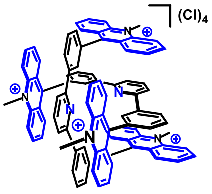 **$(1)_2^{4+}$**	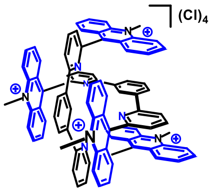 **$(2)_2^{4+}$**	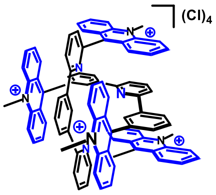 **$(1\cdot2)^{4+}$**
ΔG (kcal mol⁻¹)	-24.9	-23.0	-22.3
linker-linker distance between monomer (Å)	4.124	3.962	4.289
C_9-C_9 (Å)	7.211	7.108	7.193/7.183
[C-H···N] (Å)	2.641	2.875	3.192/2.638
torsion angle in the linker (°)	-24.5	-24.5	-24/29.4
torsion angle between both acridinium moieties (°)	-28.3	-27	27.8/-28.6

6. References

[S1] G. R. Fulmer, A. J. M. Miller, N. H. Sherden, H. E. Gottlieb, A. Nudelman, B. M. Stoltz, J. E. Bercaw, and K. I. Goldberg, *Organometallics*, **2010**, *29*, 2176–2179.

[S2] Gaussian 09, Revision D.01, M. J. Frisch, G. W. Trucks, H. B. Schlegel, G. E. Scuseria, M. A. Robb, J. R. Cheeseman, G. Scalmani, V. Barone, G. A. Petersson, H. Nakatsuji, X. Li, M. Caricato, A. Marenich, J. Bloino, B. G. Janesko, R. Gomperts, B. Mennucci, H. P. Hratchian, J. V. Ortiz, A. F. Izmaylov, J. L. Sonnenberg, D. Williams-Young, F. Ding, F. Lipparini, F. Egidi, J. Goings, B. Peng, A. Petrone, T. Henderson, D. Ranasinghe, V. G. Zakrzewski, J. Gao, N. Rega, G. Zheng, W. Liang, M. Hada, M. Ehara, K. Toyota, R. Fukuda,

J. Hasegawa, M. Ishida, T. Nakajima, Y. Honda, O. Kitao, H. Nakai, T. Vreven, K. Throssell, J. A. Montgomery, Jr., J. E. Peralta, F. Ogliaro, M. Bearpark, J. J. Heyd, E. Brothers, K. N. Kudin, V. N. Staroverov, T. Keith, R. Kobayashi, J. Normand, K. Raghavachari, A. Rendell, J. C. Burant, S. S. Iyengar, J. Tomasi, M. Cossi, J. M. Millam, M. Klene, C. Adamo, R. Cammi, J. W. Ochterski, R. L. Martin, K. Morokuma, O. Farkas, J. B. Foresman, and D. J. Fox, Gaussian, Inc., Wallingford CT, 2016.

[S3] J. P. Perdew, K. Burke, and M. Ernzerhof, *Phys. Rev. Lett.*, **1996**, *77*, 3865-3868.

[S4] F. Weigend and R. Ahlrichs, *Phys. Chem. Chem. Phys.*, **2005**, *7*, 3297-3305.

[S5] S. Miertuš, E. Scrocco, and J. Tomasi, *Chem. Phys.*, **1981**, *55* 117-129.

[S6] S. Grimme, J. Antony, S. Ehrlich and H. Krieg, *J. Chem. Phys.,* **2010**, 132, 154104.

[S7] J. Contreras-García, E. R. Johnson, S. Keinan, R. Chaudret, J.-P. Piquemal, D. N. Beratan, and Weitao Yang, *J. Chem. Theory Comput.* **2011**, *7*, 625–632.